

Anomalous Occurrence Features of the Preliminary Impulse of Geomagnetic Sudden Commencement (SC) in the South Atlantic Anomaly (SAA) region

Atsuki Shinbori¹, Yukitoshi Nishimura¹, Yuji Tsuji¹, Takashi Kikuchi¹, Tohru Araki², Akihiro Ikeda³,
Teiji Uozumi⁴, Roland E. S. Otadoy⁵, Hisashi Utada⁶, Jose Ishitsuka⁷, Nalin Baul Trivedi⁸,
Severino L. G. Dutra⁹, Nelson Jorge Schuch¹⁰, Shinichi Watari¹¹, Tsutomu Nagatsuma¹¹, Kiyohumi
Yumoto⁴

¹*Solar-Terrestrial Environment Laboratory, Nagoya University, 464-8601, Japan*

²*SOA Key Laboratory for Polar Science, Polar Research Institute of China, Shanghai 200136, China*

³*Department of Earth and Planetary Sciences, Graduate School of Science, Kyushu University, Fukuoka,*

Japan

⁴*Space Environment Research Center (SERC), Kyushu University, Fukuoka, Japan*

⁵*Department of Physics, San Carlos University*

⁶*Earthquake Research Institute, Ocean Hemisphere Research Center, Tokyo University, Tokyo, Japan*

⁷*Observatorio de Ancon, Instituto Geofisico del Peru*

⁸*Southern Regional Space Research Center (CRSPE) - INPE Universidade Federal de Santa Maria*

(UFSM) C.P. 5021 Santa Maria - RS 97110-970 Brazil

⁹*Division of Space Geophysics Brazilian National Space Research Institute Instituto Nacional de*

Pesquisas Espaciais (INPE)

¹⁰*Head Southern Regional Space Research Center - RSU/CIE/INPE - MCT Santa Maria RS Brazil*

¹¹*National Institute of Information and Communications Technology, Tokyo, 184-8795, Japan*

Abstract

Occurrence features of the preliminary impulse (PI) of geomagnetic sudden commencement (SC) both in the Pacific Ocean and South Atlantic Anomaly (SAA) regions were investigated using the long-term magnetic field data obtained from the Circum-pacific Magnetometer (CPMN) and NICT Space Weather Monitoring (NSWM) magnetometer networks. The low-latitude preliminary reverse impulse (PRI) at Okinawa (OKI: dip latitude = 37.97°) in the Pacific Ocean region appeared in all the magnetic local time (MLT) sectors with the peak occurrence rate of 40 % around noon. On the other hand, the PRI occurrence rate at Santa Maria (SMA: dip latitude = -34.35°) near the center of the

SAA region, showed a significant enhancement in the daytime sector (08-16 h, MLT) with the peak value of 80 %, which resembles the occurrence feature of the equatorial PRI. Moreover, the PRI amplitude around noon at SMA was about 3.0 times larger than that at OKI. From the calculation of the ionospheric conductivity derived from the IRI-2007 and NRLMSISE-00 models, it is shown that the height-integrated conductivity was more enhanced in the SAA region (SMA), where the ambient magnetic field intensity is weak, compared with that in the Pacific Ocean region (OKI). Therefore, the anomalous increase of the PRI occurrence and amplitude is caused by the significant enhancement of the ionospheric conductivity due to the weakness of the ambient magnetic field intensity in the SAA region.

1. Introduction

The geomagnetic sudden commencement (SC) is characterized by a sudden increase of the H-component of magnetic field in low latitudes on the ground within ten minutes. This phenomenon is caused by an abrupt enhancement of the Chapman-Ferraro current in the dayside magnetopause associated with the sudden magnetospheric compression, which is triggered by a rapid enhancement of solar wind dynamic pressure related to interplanetary

shocks or discontinuities. The enhanced Chapman-Ferraro current produces a step-like increase of northward magnetic field in the magnetosphere [e.g., Kokubun, 1983; Kuwashima and Fukunishi, 1985], plasmasphere [Shinbori et al., 2004] and on the ground [e.g., Araki, 1977]. However, the ground magnetic field signature of step-like increase is seen only in low latitudes of less than 20° (geomagnetic latitude: GMLAT) [e.g., Matsushita, 1962; Araki, 1977, 1994; Russell et al., 1992]. The waveform of magnetic field signatures during SC shows two-pulse structure, consisting of the preliminary impulse (PI) with its duration time of ~ 1 minute followed by the main impulse (MI). The occurrence feature and amplitude of the PI and MI signatures strongly depend on magnetic latitude and local time [e.g., Nagata, 1952; Matsushita, 1962; Rastogi and Sastri, 1974; Araki, 1977, 1994; Araki et al., 1985; Tsunomura, 1998, 1999; Kikuchi et al., 2001; Shinbori et al., 2009]. At high latitude in the afternoon sector, a preliminary reverse impulse (PRI) frequently appears with its duration time of about 1 minute before the onset of an MI signature, while a preliminary positive impulse (PPI) is observed in the morning sector [e.g., Nagata, 1952; Matsushita, 1962; Araki, 1977; Kikuchi and Araki, 1985]. The amplitude of the PRI and PPI signatures tends to decrease with decrease of magnetic latitude [Nagata, 1952], and these magnetic signatures were rarely detected at low latitudes of less than 20° (GMLAT) [Matsushita,

1962; Araki, 1977, 1994]. However, the PRI signature appears at the daytime magnetic equator, again, simultaneously with the high-latitude PRI in the afternoon sector. The occurrence rate of the PRI maximizes around local noon [e.g., Rastogi and Sastri, 1974; Araki, 1977]. Rastogi and Sastri [1974] reported that the occurrence rate of the equatorial PRI strongly depends on the dip latitude. The global morphology of the PRI signature has been explained by the magnetic effects of two-cell ionospheric currents driven by a dusk-to-dawn electric field which is imposed on the polar ionosphere carried by field-aligned currents (FACs) [e.g., Araki, 1977, 1994; Kikuchi et al., 2001; Sastri, 2002]. The dusk-to-dawn electric field propagates instantaneously to the magnetic equator where it generates the westward ionospheric currents to produce the PRI signature on the ground. On the other hand, an MHD simulation of the magnetospheric response to solar wind impulse gives comprehensive information on the FACs and ionospheric current system generated during the PI phase [e.g., Slinker et al., 1999; Fujita et al., 2003a, 2003b].

It has been known from earlier studies that the PPI and PRI pulses are frequently observed in the morning and afternoon sectors, respectively, of the middle-latitude region from 55° to 20° (GMLAT). The PRI occurrence rate decreases abruptly with decrease of magnetic latitude from 49.0° to 29.2° [e.g., Nagata, 1952; Matsushita, 1962; Yamada et al.,

1997]. Kikuchi et al. [2001] demonstrated that the PPI signature frequently appears at middle latitudes in the afternoon sector during winter season while the morning PPI occurrence does not depend on season. They pointed out that the magnetic effects produced by the FACs play a major role in the afternoon PPI at middle latitudes, based on the results of model calculation proposed by Tsunomura and Araki [1984]. In recent studies, the magnetic effects of the FACs have been applied for the physical mechanism of the nighttime enhancement of SC amplitude in the middle and low latitudes during an MI phase [Araki et al., 2006, 2009; Shinbori et al., 2009].

The PPI signature in the nighttime sector of the dip equator also appears simultaneously with the PRI one in the daytime sector. Araki et al. [1985] found that there are two kinds of magnetic field perturbations associated with SCs in the nighttime sector, based on the results of rapid-run magnetograms from Guam (GUM, GMLAT=5.2° N): one is the ordinary waveform of magnetic field variations during SCs with a simple step-like increase in the H-component, and another is with two step-like magnetic field variations. The latter has been called 'Stepwise SC'. The maximum occurrence of the Stepwise SC was at 03:00 (MLT). Araki et al. [1985] interpreted this occurrence feature of the nighttime Stepwise SC as the magnetic effects of the eastward ionospheric currents driven by the dusk-to-dawn

electric field penetrated to the equatorial ionosphere in the nighttime sector. Using high-resolution (1 second) geomagnetic field data obtained at Jicamarca (JIC, GMLAT=0.0°) in a period from 1998 to 2005, Han and Li [2008] showed that the occurrence rate of the PPI/Stepwise SC events in the dawn sector (04-07 h, MLT) was clearly higher than that in the nighttime sector (22-03 h, MLT). From the occurrence feature of the PPI/Stepwise SC, they suggested that the dawn-time enhancement of the PPI/Stepwise at the magnetic equator reflects the magnetic effects of the ionospheric currents and FACs.

In the South Atlantic Anomaly (SAA) region, total geomagnetic field F has been known to be depressed significantly ($F \sim 23000$ nT), compared with the averaged total field ($F \sim 40000$ nT) on the Earth's surface. Due to the low field intensity over the SAA region, the trapped and azimuthally drifting energetic particles originating from the inner radiation belt, bouncing between hemispheres, precipitate deeply into the ionosphere and atmosphere [e.g., Macdonald and Walt, 1962; Vernov et al., 1967; Tsurutani and Lakhina, 1997]. The particle precipitation results in the enhanced ionospheric conductivity at the altitude of D- and E-region due to increase of ionization during both the quiet and disturbed periods suggested by observations of the Ionosonde, riometer, and VLF radio propagation [e.g.,

Abdu et al., 1973; Nishino et al., 2002]. Abdu et al. [1998, 2003a, b] reported that the ionospheric conductivity tends to be more enhanced during the disturbed periods than during the quiet ones. The anomalous ionization and new finding of the associated electrodynamic in the SAA region near the magnetic equator have in detail been reviewed in the paper of Abdu et al. [2005]. Recently, Trivedi et al. [2005] reported that the SC amplitude during the MI phase tends to be more enhanced near the center of the SAA region than in the other regions, based on the analysis results of 37 SC events. They interpreted this observation as an intensification of ionospheric currents due to the enhancement of ionospheric conductivity associated with the precipitation of electrons and ions from the inner radiation belt into the atmosphere of the SAA region.

In the present data analysis of the long-term observations with high time resolution of 1 or 3 second, we found that well-defined magnetic field signatures of the PRI and PPI frequently appeared at the Santa Maria station (SMA, GMLAT=-19.82°; dip latitude=-34.35°) located near the center of the SAA region. This magnetic field signature in low latitudes during SC is quite different from that shown in the past studies [e.g., Matsushita, 1962; Araki, 1977, 1994]. In this paper, we first present the difference between the PRI and PPI occurrence features during SCs in the SAA and Pacific Ocean regions from

the dip equator to low latitudes by analyzing a large number of SC events occurred within a period from 1996 to 2008. Based on the above results, we clarify a cause of the different occurrence feature of the PRI and PPI signatures in the SAA region using ionospheric conductivity deduced from the IRI-2007 [Bilitza and Reinisch, 2008] and NRLMSISE-00 [Picone et al., 2002] models.

2. Observation Data

2-1. Identification of SC events

Using the SYM-H index [Iyemori, 1990; Iyemori and Rao, 1996] with high time resolution of 1 minute, we first identified the magnetic field signature of an abrupt increase with its amplitude of more than 5 nT within 10 minutes in the SYM-H index. In this case, 3786 events of the magnetic field disturbance are found in a long period from January 1996 to December 2008. Since the SYM-H index is deduced from averaging magnetic field disturbances of the H-component obtained from 6 stations which are located in the middle-latitude region with approximately equal longitudinal span, magnetic field effects of the ionospheric DP 2-type currents may be eliminated as already described in the paper of Araki et al. [1993]. They demonstrated that the upper envelope in the scatter plot of the Dst

index depends mainly on the square root of solar wind dynamic pressure jump. Therefore, we can say that the magnetic field disturbances of a sudden increase in the SYM-H index are related to the enhancement of the Chapman-Ferraro current due to the sudden compression of the magnetosphere. However, the above criterion possibly includes other geomagnetic disturbances such as an abrupt increase of the H-component geomagnetic field during the early recovery phase of geomagnetic storms or positive bay phenomena associated with the onset of substorms. In order to exclude these magnetospheric phenomena, we checked whether there is a sudden enhancement of solar wind dynamic pressure in the solar wind corresponding to a sudden increase event in the SYM-H index or not. Here, we referred the solar wind and IMF data obtained from the IMP-8, Geotail, ACE and Wind satellites. These data were provided from the CDAWeb site (<http://cdaweb.gsfc.nasa.gov/>). In particular, for exclusion of positive bay phenomena associated with the onset of substorms, we identified Pi 2 magnetic pulsations [e.g., Saito et al., 1976] at the onset of a sudden increase of the SYM-H value. In this data analysis, we used ground magnetic field data with high-time resolution of 1 or 3 seconds obtained from the low-latitude stations belonging to the Circum-Pan-Pacific-Magnetometer-Network (CPMN) [Yumoto and the CPMN Group, 2001] and NICT Space Weather Monitoring

(NSWM) [Kikuchi et al., 2008] operated by Kyushu University and NICT, respectively. As a result, we could identify 3163 events of the magnetic field disturbance purely related to a sudden enhancement of solar wind dynamic pressure in a period from January 1996 to December 2008. In the present study, we defined the magnetic field signature as SC.

2-2. Station data and definition of the PI and MI signatures

For each SC event identified by the above method, the precise onset time, duration time and amplitude of the PI and MI signatures were identified by referring geomagnetic field variations of the H-component from the rapid sampling records with the time resolution of 1 or 3 seconds. The rapid sampling data were obtained from 9 stations of Ancon (ANC, 11.79S, 77.16W geographic coordinates (GR), 3.10N, 354.66E geomagnetic coordinates (GM)), Sao Luis (SLZ, 2.60S, 44.20W GR, 6.49N, 27.75E GM), Eusebio (EUS, 3.85S, 38.42W GR, 4.72N, 33.41E GM), Santa Maria (SMA, 29.72S, 53.72W GR, 19.82S, 13.31E, GM) Okinawa (OKI, 24.75N, 125.33E GR, 16.87N, 198.41E GM), Cebu (CEB, 10.35N, 123.91E GR, 0.85N, 195.27E GM), Pohnpei (PON, 7.00N, 158.33E GR, 0.27N, 229.44E GM), Guam (GAM, 13.59N, 144.87E GR, 5.30N, 215.64E GM), and Yap (YAP, 9.49N, 138.09E GR, 0.38N, 209.21E GM) located from the low latitudes to equator in the Pacific

and SAA regions. The OKI, GAM, YAP, SLZ and SMA stations belongs to NSWM, while the ANC, EUS, SMA, CEB, and PON ones is a part of CPMN. Table 1 presents the data analysis period and the number of SC events for each station.

In the present analysis, we defined a negative impulse with its amplitude of more than 0.1 nT as a PRI signature, which precedes an abrupt increase of the H-component during SCs. The PRI amplitude is identified as the difference between the geomagnetic field levels of the H-component before the PRI onset and at the time when the minimum was recorded. On the other hand, for determination of the PPI signature, which frequently appears at the nighttime equator and at the low and middle latitudes of the morning sector, we identified a stepwise magnetic signature of the H-component during SCs reported by Araki et al. [1985].

3. Examples of SC events

3-1. 21 October 2001 SC

Figure 1 shows magnetic field variations of the H-component in both the SAA and Pacific Ocean regions associated with SC occurred at 16:47:45 (UT) on 21 October, 2001. The upper and lower panels indicate the H-component data with the time resolution of 1

second obtained at the ANC, EUS and SMA stations in the SAA region and at the OKI, GAM, CEB, YAP, and PON stations in the Pacific Ocean region, respectively. The time interval is 7 minutes from 16:46 to 16:53 (UT). The vertical dashed lines in both the panels give the onset time of SC, while the dotted-dashed line in the lower panel indicates the peak amplitude of the PPI/Stepwise signature [Araki et al., 1985] associated with SC. In this case, the SAA and Pacific Ocean regions are located in the noon (12-13 h, MLT) and midnight (1-2 h, MLT) sectors, respectively. The upper panel in Figure 1 shows that a distinctive PRI magnetic field signature appeared at all the stations in a region from the low latitude (dip latitude: -34.35°) to the equator (dip latitude: 1.43°) in the SAA region about 1 minute before the beginning of the MI signature. The PRI signature started simultaneously at 16:47:45 (UT) at all the stations. The maximum PRI amplitudes at ANC, EUS and SMA are recorded as 64.72 nT, 8.55 nT and 24.83 nT at 16:48:19, 16:48:13 and 16:48:12 (UT), respectively. It is quite evident from this result that the PRI amplitude at SMA (dip latitude: -34.35°) in the low latitude is about three times larger than that at EUS (dip latitude: -11.99°) near the magnetic equator. Therefore, this PRI occurrence and amplitude are quite different from that obtained from the past studies, which showed that the PRI signature can rarely be observed in the dip latitudes of more than 15° [e.g., Matsushita, 1962; Araki, 1977,

1994].

On the other hand, the lower panel in Figure 1 shows that a step-like or stepwise variation of the H-component appears at the SC onset with its amplitude of 27-42 nT in the Pacific Ocean region of the nighttime sector. The onset time was almost coincident with that of the PRI signature in the SAA region of the daytime sector. Especially, the magnetic signature of the H-component at PON and YAP near the equatorial region showed a PPI/Stepwise variation indicated by the vertical dotted-dashed line at 16:48:17 (UT). This signature can not clearly be seen in the waveform of magnetic field variation at OKI in the low-latitude region. This result indicates that the magnetic field variation at OKI mainly consists of the magnetic disturbances produced by the Chapman-Ferraro and field-aligned currents [e.g., Araki, 1977; Shinbori et al., 2009].

In order to confirm the PPI/Stepwise signature near the equatorial region associated with SC, we subtracted the magnetic field variation of the H-component at OKI from that detected at each equatorial station (GAM, CEB, YAP and PON). Then, we added latitude correction to the magnetic field variation at OKI in this calculation. Figure 2 shows the equatorial magnetic field variation of the H-component subtracted from that at OKI during SC. The format of this figure is the same as that of the panel (b) in Figure 1. In Figure 2, the

magnetic field signatures at GAM, YAP, and PON shows a rapid increase with its duration time of 49-62 seconds around 16:47:44 (UT) after the onset of SC, corresponding to the PPI/Stepwise waveform. The onset time of the PPI/Stepwise signature is almost coincident with that of the daytime PRI detected in the SAA region. The maximum PPI amplitudes at GAM, YAP and PON are recorded as 6.38 nT, 2.62 nT and 6.92 nT at 16:48:25, 16:48:13 and 16:48:13 (UT), respectively. This magnetic signature has been thought as the magnetic effect of eastward ionospheric current driven by the dusk-to-dawn electric field [Araki et al., 1985, Han and Li, 2008 and Kikuchi et al., 2009]. After the PPI/Stepwise signature, magnetic pulsation with its period of 56-102 seconds appears for about 2-3 minutes at the three equatorial stations (PON, YAP and GAM).

3-2. 4 November 2003 SC

Figure 3 shows magnetic field variations of the H-component associated with SC occurred at 06:25:51 (UT) on 4 November, 2003. The upper and lower panels indicate the H-component data with time resolution of 1 second obtained at the SLZ, EUS and SMA stations in the SAA region and at the OKI, CEB, YAP, and PON stations in the Pacific Ocean region, respectively. The time interval is 7 minutes from 06:24 to 06:31 (UT). The

vertical dashed lines in both the panels give the onset time of SC, while the dotted-dashed line in the upper panel indicates the peak amplitude of the PPI/Stepwise signature associated with SC. In this case, the SAA and Pacific Ocean regions are located in the pre-dawn (03-04 h, MLT) and afternoon (15-16 h, MLT) sectors, respectively. In the upper panel in Figure 3, a distinctive PPI/Stepwise magnetic field signature appeared at all the stations in a region from the low latitude to the equator near the SAA region. The PPI/Stepwise signature started simultaneously at 06:25:51 (UT) at all the stations. The maximum PPI/Stepwise amplitudes at SLZ, EUS and SMA are recorded as 9.94 nT, 11.01 nT and 4.80 nT at 06:26:09, 06:26:10 and 06:26:05 (UT), respectively. In this case, the PPI/Stepwise amplitude at SMA in the low latitude becomes the smallest. Moreover, comparing the waveform of magnetic field variation at OKI during SC shown in the lower panel in Figure 1, the low-latitude PPI/Stepwise signature can be seen more distinctively at SMA.

On the other hand, the lower panel in Figure 3 shows that a PRI magnetic signature of the H-component appeared distinctively at the SC onset at all the stations in the afternoon sector of the Pacific Ocean regio. The onset time was almost coincident with that of the PPI/Stepwise signature in the pre-dawn sector of the SAA region. The maximum PRI

amplitudes at OKI, CEB YAP and PON are recorded as 1.34 nT, 5.80 nT, 5.62 nT and 4.36 nT at 06:25:58, 06:26:05, 06:26:06 and 06:26:06 (UT), respectively. The PRI amplitude and period at OKI in the low latitude (dip latitude: 37.97°) become the smallest and shortest in the Pacific Ocean region. However, this observational result suggests that the PRI signature can be observed even in the dip latitude of more than 15° . This fact is not consistent with the result of Matsushita [1962] and Araki [1977 and 1994]. Moreover, comparing the waveform of magnetic field variation at SMA shown in the upper panel in Figure 1, the PRI amplitude at SMA is about 8.5 times larger than that at OKI. This result indicates that there is a distinctive difference between the PRI responses at OKI and SMA although both the stations are located near the same magnetic latitude. In the next section, we will verify the difference of the PRI and PPI/Stepwise occurrence in between the Pacific Ocean and SAA regions, based on the statistical analysis result.

4. Statistical Study

In this section, we show the statistical analysis result of occurrence features of the PRI and PPI/Stepwise signatures during SCs from the dip equator to low latitudes in both the Pacific Ocean and SAA regions. In the present analysis, we used the long-term

geomagnetic field data obtained from the 6 stations (ANC, EUS, GAM, OKI, PON, SLZ, SMA and YAP). The number of SC events and analyzed period for each station are presented in Table 1.

4.1 Occurrence rate of the PRI and PPI/Stepwise signatures during SC

Figure 4 shows an occurrence rate of the PRI and PPI/Stepwise signatures during SCs detected at 8 stations as a function of magnetic local time. The left and right panels are that of the Pacific Ocean and SAA regions, respectively, in a dip latitude range from 1.0° to 38° . The red (PRI), blue (PPI) and green (Non) colors correspond to the occurrence rate of the PRI, PPI/Stepwise and unclear signatures, respectively. The station name and dip latitude are shown in the top of each panel. The dip latitude is calculated from the IGRF-10 model at the altitude of 120 km in the ionosphere above each station. In the left panels (a)-(d) in Figure 4, most of the PRI and PPI signatures in the Pacific Ocean region tend to appear dominantly in the daytime (06-18 h, MLT) and nighttime (18-06 h, MLT) sectors, respectively. The occurrence rate decreases with increase of dip latitude. Especially, the peak value of the PRI around noon decreases abruptly from 100 % (PON) to 40 % (OKI). The equatorial PRI signature at PON and YAP tends to appear up to the post-dusk or pre-midnight sector (\sim 21-22 h, MLT) with its

occurrence rate of more than 10 %. The occurrence feature of the equatorial PRI signatures well agrees with the results of the past studies by Matsushita [1962] and Araki [1977]. However, the fact that the PPI/Stepwise occurrence rate reaches the maximum in the midnight sector (23-01 h, MLT) is a bit different from that reported by Araki et al. [1985] and Han and Li [2008].

In the right panels (e)-(h) in Figure 4, most of the PRI and PPI signatures in the SAA region tend to appear dominantly in the daytime (06-18 h, MLT) and nighttime (18-06 h, MLT) sectors, respectively. This tendency is almost the same as that in the Pacific Ocean region. However, the occurrence rate does not almost change with increase of dip latitude. The peak value of the PRI around noon decreases slightly from 94 % (ANC) to 80 % (SMA). The occurrence rate at EUS and SMA in the SAA region is larger than that at GAM and OKI in the Pacific Ocean region in spite of almost the same dip latitude. Especially, it should be noted that the PRI occurrence rate at SMA is twice as large as that at OKI around noon. The occurrence feature of the low-latitude PRI signatures is quite different from the results of the past studies by Matsushita [1962] and Araki [1977].

4.2 Local time dependence of the PRI amplitude

Figure 5 shows an averaged distribution of the PRI amplitude at the dip equator (panel (a)) and off equator (panel (b)) as a function of magnetic local time. The red and green curves are the PRI amplitude observed in the Pacific Ocean and SAA regions, respectively. The value of each point is 3-hour running average. In the panel (a) in Figure 5, the equatorial PRI amplitude enhances significantly in the daytime sector (06-18 h, MLT) due to an enhancement of the ionospheric current driven by the dusk-to-dawn polar electric field by the Cowling effect [Hirono, 1952]. This amplitude reaches the maximum value of 7.7 nT around 10 h (MLT). In this case, the local time dependence of the PRI amplitude does not show a clear difference between in the Pacific Ocean (PON) and SAA (ANC) regions.

On the other hand, as shown in the bottom panel (b) in Figure 5, the local time dependence of the PRI amplitude show a clear difference between in the Pacific Ocean (OKI) and SAA (SMA) regions. The most pronounced point is that the PRI amplitude at SMA enhances significantly in a region from the daytime to evening sectors (05-23 h, MLT), compared with that at OKI. The PRI amplitude reaches the maximum around noon both at SMA and OKI. This value at SMA is about three times larger than that at OKI. The second point is that the PRI amplitude at OKI enhances slightly around midnight. This

feature can not be seen in the averaged curves at SMA and equatorial stations (PON and ANC). This nighttime PRI signature at OKI can be thought as the magnetic effects of the FACs flowing out and into the dawn and dusk polar ionosphere, respectively. The FACs manifest the equatorward magnetic field disturbance in the low and middle latitudes of the nighttime sector, based on the result of Kikuchi et al. [2001].

5. Discussion

5.1 Occurrence features of the low-latitude PRI at OKI

In the past studies, it has been believed that the PRI signature associated with SC can rarely be detected in low latitudes of less than 20 degrees (GMLAT) [e.g., Matsushita, 1962; Araki, 1977]. Araki [1977] showed that only 5 of 343 SC events at Honolulu in the low latitude indicate a PRI signature in the SC waveform of the H-component within a period from July 1957 to December 1967. In this case, the occurrence rate of the PRI signature becomes about 1-2 %. However, the present statistical analysis result showed that the PRI signature appears with its maximum occurrence rate of approximately 40 % around noon at OKI (37.97° , dip latitude; 16.87° , GMLAT) as shown in the panel (d) in Figure 4. This value is about twenty times larger than that shown in the past studies. The significant

enhancement of the low-latitude PRI occurrence can be considered as the following two reasons. One is a significant improvement of the magnetometer with high accuracy, which can detect a weak signature of magnetic field. In the present analysis, the daytime PRI amplitude at OKI was in a range from 0.22 nT to 0.51 nT. The other is digitization of the observation data. This enables us to easily analyze a magnetic field phenomenon with several criteria.

The characteristics of the low-latitude PRI signature at OKI indicate that the PRI amplitude tends to enhance around noon and midnight, while the occurrence rate in the daytime sector was larger than in the nighttime sector. It reaches the maximum value of 40 % around noon. This daytime enhancement, which shows that the PRI tends to appear dominantly in the daytime sector, is almost similar to that near the equatorial stations (for example, PON and ANC) except for the following two points; one is that the occurrence rate decreases with increase of the dip latitude. The other is that the peak location of the PRI amplitude at the dip equator shifts to the morning sector (~ 10 h, MLT), compared with that at the off equator. From the above result, it can be inferred that the low-latitude PRI in the daytime sector is produced by ionospheric currents (the Pedersen or Hall current) driven by a dusk-to-dawn polar electric field [Araki, 1977, 1994; Kikuchi et al., 2001]. Kikuchi et

al. [1985] verified that the dusk-to-dawn electric field originating in the polar ionosphere penetrates to the low-latitude ionosphere associated with an SC, based on the HF Doppler and magnetic field observations with high time resolution.

On the other hand, as shown in the panel (d) in Figure 4, the low-latitude PRI signature also appears in the nighttime sector (18-06 h, MLT) with its averaged occurrence rate of 10 % (less than in the daytime sector). The nighttime PRI amplitude tends to enhance slightly with a peak around midnight. This occurrence feature of the nighttime PRI is in agreement with the southward magnetic field variation produced by the FACs flowing into and out the dusk and dawn polar ionosphere [Kikuchi et al., 2001]. Since the ionospheric conductivity in the nighttime sector is much lower than that in the daytime one, the ground magnetic field variation due to the FACs becomes dominant as predicted by the model calculation result [Kikuchi et al., 2001].

5.2 Characteristics of the equatorial PRI

The earlier statistical study of the PRI occurrence near the equatorial region showed that (1) most of the PRI tend to appear dominantly in the daytime sector (06-18 h, LT) with a peak occurrence rate around noon (12-13 h, LT) and (2) the maximum occurrence rate is

50 % at Guam (dip latitude: 12.1°) and 75 % at Koror (dip latitude: -0.1°) [Araki, 1977]. Rastgi and Sastri [1974] also showed that occurrence rate of the equatorial PRI is approximately 50 % at midday from the original normal-run magnetogram at Kodaikanal (dip latitude: 3.0°). In the present analysis, the occurrence feature of the equatorial PRI was in agreement with that of the above works, and did not show a remarkable difference of the PRI occurrence between the Pacific Ocean (PON, YAP) and SAA (ANC, SLZ) regions as shown in Figure 4. However, the peak value of the occurrence rate around noon becomes larger than that of the above works. Especially, it reaches 100 % at PON near almost the dip equator. The enhancement of the PRI occurrence in the equatorial region is due to a significant improvement of the magnetometer with high accuracy and the definition of the PRI phenomena. In the present study, the PRI signature was defined as a negative impulse with its amplitude of more than 0.1 nT as already described in section 2. Moreover, in the past studies [e.g., Matsushita, 1962; Araki, 1977], since a rapid-run magnetogram was usually used to identify the PRI waveform associated with SCs, it seems that a detailed analysis of magnetic field variations with a small amplitude can not be conducted.

The occurrence of the PPI/Stepwise signature in the nighttime sector concentrates in a local time range of 22-05 h (LT: local time) with its maximum occurrence rate of 50 % at

03 h (LT) [Araki et al., 1985]. Han and Li [2008] found that the occurrence rate of the PPI enhances in the dawn sector (05-07 h, LT) using geomagnetic field data obtained at Jicamarca (dip latitude: 1.5 degrees). They interpreted the dawn enhancement of the PPI occurrence as the magnetic effects produced by both the ionospheric currents and field-aligned currents (FACs), based on the model calculation result of Kikuchi et al. [2001]. However, in the present study, the occurrence feature of the PPI/Stepwise signature did not show a predawn or dawn enhancement of the occurrence rate near the dip equatorial stations (PON and ANC) pointed out by Araki et al. [1985] and Han and Li [2008]. Instead, the occurrence rate became the maximum around midnight (23-01 h, MLT).

5.3 Enhancement of the low-latitude PRI in the SAA region (SMA)

As already shown in the panel (h) in Figure 4, the occurrence rate of the PRI and PPI/Stepwise signatures was enhanced significantly at SMA near the center of the SAA region, compared with that at OKI in the Pacific Ocean region. The peak occurrence of the PRI signature at SMA is twice as large as that at OKI around noon. The PRI amplitude at SMA was also enhanced significantly with the peak value of 1.5 nT around noon, which is three times larger than at OKI as shown in the panel (b) in Figure 5. Moreover, this

occurrence distribution of the PRI signature is almost the same as that in the equatorial region (for example, ANC and EUS) although the maximum occurrence rate at SMA is a little smaller than near the dip equator. This fact indicates that both the equatorial and low-latitude PRI are produced by ionospheric currents driven by the dusk-to-dawn polar electric field. Therefore, the enhancement of the PRI amplitude at SMA suggests that the ionospheric conductivity in the SAA region tends to be much higher than that in the other regions.

In order to verify whether the ionospheric conductivity near the center of the SAA region is higher than that in the Pacific Ocean region, we calculated the height-integrated ionospheric conductivity at 4 stations (PON, OKI, ANC and SMA), based on the International Reference Ionosphere 2007 (IRI-2007) [Bilitza and Reinisch, 2008] and NRLMSISE-00 [Picone et al., 2002] models. The IRI is an empirical standard model of the ionosphere, based on all available data sources (the powerful incoherent scatter radars (Jicamarca, Arecibo, Millstone Hill, Malvern, and St. Santin), the ISIS and Alouette topside sounders, and in situ instruments on several satellites and rockets). This empirical model provides monthly averages of the electron density, electron temperature, ion temperature, and ion composition in the altitude range from 50 km to 2000 km for given location, time

and date. The NRLMSISE-00 is an empirical and global model of the Earth's atmosphere from ground to space. 'NRL' and 'MSIS' stand for the US Naval Research Laboratory and Mass Spectrometer and Incoherent Scatter Radar, respectively. 'E' of NRLMSISE indicates that the model extends from the ground through exosphere and 00 is the year of release. This model provides the composition of the neutral atmosphere, total mass density and temperature for given location as input parameters: date, time, local apparent solar time, 81 day average of F10.7 solar flux, daily magnetic index, altitude geodetic latitude and geodetic longitude. We also used the IGRF-10 model in order to obtain the cyclotron frequencies of each particle species. In the present calculation, we adapted two-dimensional thin shell model of the ionospheric conductivity described in the paper of Tsunomura [1999, 2000]. Since the ionosphere takes the form of spherical shell, the polar co-ordinate system (θ, ϕ, z) is usually used to describe the physical process. The axis z directs vertically upward. The non-diagonal components in the conductivity tensor are caused by the Hall conductance in the ionosphere. The components of the ionospheric conductivity tensor are derived by a simple algebraic calculation on the assumption of the null vertical current. The forms of $\sigma_{\theta\theta}$, $\sigma_{\theta\phi}$, and $\sigma_{\phi\phi}$ are

$$\sigma_{\theta\theta} = \frac{\sigma_{\parallel}\sigma_P}{\sigma_{\parallel}\sin^2 I + \sigma_P\cos^2 I} \quad (1)$$

$$\sigma_{\theta\phi} = \frac{\sigma_{\parallel}\sigma_H\sin I}{\sigma_{\parallel}\sin^2 I + \sigma_P\cos^2 I} \quad (2)$$

and

$$\sigma_{\phi\phi} = \sigma_P + \frac{\sigma_H^2\cos^2 I}{\sigma_{\parallel}\sin^2 I + \sigma_P\cos^2 I} \quad (3)$$

where σ_{\parallel} , σ_P , and σ_H are longitudinal, the Pedersen and Hall conductivities and I is dip latitude, respectively. The dip latitude is calculated from the IGRF-10 model. $\sigma_{\theta\phi}$ is exactly minus of $\sigma_{\phi\theta}$. The equation of Ohm's law for the height-integrated ionospheric current is written as

$$\begin{pmatrix} J_{\theta} \\ J_{\phi} \end{pmatrix} = \begin{pmatrix} \Sigma_{\theta\theta} & \Sigma_{\theta\phi} \\ \Sigma_{\phi\theta} & \Sigma_{\phi\phi} \end{pmatrix} \cdot \begin{pmatrix} E_{\theta} \\ E_{\phi} \end{pmatrix} \quad (4)$$

where J_{θ} , J_{ϕ} , E_{θ} and E_{ϕ} are the components of the height-integrated current density and electric field, respectively. Each component of Σ is the height-integrated value of $\sigma_{\theta\theta}$, $\sigma_{\theta\phi}$, $\sigma_{\phi\theta}$ and $\sigma_{\phi\phi}$. The integration range is obtained from the width of dynamo layer in an averaged altitude range from 90 km to 150 km, where the ionospheric current flows. This dynamo layer is derived from the relationship between the collision and cyclotron frequencies for each component.

Figure 6 shows altitude profiles of ionospheric conductivity (panels (a) and (b)), and collision and cyclotron frequencies (panels (c) and (d)) at OKI and SMA at local magnetic noon (12 h, MLT) on September 23, 2002. The vertical axes in each panel are altitude in a range from 50 to 250 km. The red, blue, and green lines in the panels (a) and (b) indicate the $\sigma_{\theta\theta}$, $\sigma_{\theta\phi}$, and $\sigma_{\phi\phi}$ conductivities at OKI and SMA, respectively. The labels ‘Nu_NO+n’, ‘Nu_O+n’, ‘Nu_en’, ‘ Ω_{ce} ’, ‘ Ω_{ci} ’, ‘ Ω_{ce} ’, ‘ Ω_{ci} ’, ‘ ν_{en} ’, ‘ ν_{in} ’ and ‘ ν_{in} ’ indicated by each line color stand for the collision frequencies between the neutral particles and ions (NO^+ , O^+) and electron, and the cyclotron angular frequencies of electron, NO^+ and O^+ ions, respectively. The region between two dashed lines is dynamo layer satisfying $\nu_{en} < \Omega_{ce}$ and $\Omega_{ci} < \nu_{in}$. Here, Ω_{ce} , Ω_{ci} , ν_{en} , and ν_{in} are electron, ion cyclotron angular frequencies, electron-neutral and ion-neutral collision frequencies, respectively. In the present calculation, we determined the upper limit of dynamo layer as the cross point between the NO^+ ion cyclotron angular frequency and NO^+ ion-neutral collision frequency. In the panels (a) and (b) in Figure 6, all the components of the $\sigma_{\theta\theta}$, $\sigma_{\theta\phi}$, and $\sigma_{\phi\phi}$ conductivities at SMA tends to be enhanced significantly, compared with those at OKI. For example, the peak value of the $\sigma_{\phi\phi}$ component at the altitude of 126 km at SMA is twice as large as that at OKI. This result suggests that the ionospheric conductivity in the center of the SAA region tends

to be larger than that in the Pacific Ocean region. Since the electron density profile at SMA is almost the same as that at OKI in the equinox season, the enhancement of the ionospheric conductivity in the center of the SAA region can be caused by weakness of the ambient magnetic field intensity. As a next step, to derive the height-integrated conductivities above 4 points (ANC, OKI, PON, and SMA), we determined the height-integrated range by identifying dynamo layer indicated by the region between the two dashed lines in the panels (c) and (d) in Figure 6. In this case, the height-integrated ranges are 72-126 km and 77-132 km at OKI and SMA, respectively. It should be noted that the dynamo layer at SMA moves the upper ionosphere of higher plasma density region with the distance of 5 km. The upward movement of the dynamo layer causes a significant increase of the ionospheric current intensity produced by the ground magnetic field variations. From the above consideration, an anomalous enhancement of the low-latitude PRI and PPI/Stepwise signatures associated with an SC is mainly caused by the large enhancement of ionospheric conductivity due to weakness of the ambient magnetic field and the associated extension of the dynamo layer in the SAA region.

Moreover, in order to demonstrate that the enhancement of the low-latitude PRI amplitude is mainly due to the enhanced ionospheric conductivity in the SAA region, we

compared the ratio of the PRI amplitude at SMA to OKI with that of the height-integrated conductivity. Figure 7 shows the ratios (ANC/PON and SMA/OKI) of the daytime PRI amplitude and height-integrated conductivity as a function of magnetic local time. In this case, we calculated the ratio of the $\Sigma_{\phi\phi}$ component in the conductivity tensor, which relates to the J_{ϕ} and E_{ϕ} components of the ionospheric current and electric field, respectively, because this component corresponds to the Cowling conductivity at the dip equator. In each panel, the red and green lines indicate the height-integrated conductivity and PRI amplitude ratios, respectively. The upper panel (a) shows that both the conductivity and PRI amplitude ratios (ANC/PON) at the dip equator are almost constant for magnetic local time except for the evening sector (16-18 h, MLT). The value of the conductivity ratio is 1.6 times larger than that of the PRI amplitude one. This result indicates that the E_{ϕ} component of the equatorial electric field at ANC can be slightly smaller than that at PON, and that the intensity of the E_{ϕ} component depends on geomagnetic longitude. On the other hand, the bottom panel (b) shows that the value of the conductivity ratio (SMA/OKI) is almost the same as that of the PRI amplitude ratio. The difference value was 0.5 of 2.5-3.6 around the noon sector (08-16 h, MLT), which corresponds to 14-20 % of the conductivity ratio for each magnetic local time. Therefore, it can be concluded that the enhancement of the

low-latitude PRI amplitude at SMA located near the center of the SAA region is mainly due to the ionospheric conductivity enhancement associated with weakness of the ambient magnetic field intensity.

Although the present study showed that a significant enhancement of ionospheric conductivity leads to weakness of the ambient magnetic field in the SAA region, several past studies of ionospheric environment over this region have pointed out the precipitation effect of energetic particles originating from the inner radiation belt deeply into the ionosphere and atmosphere [e.g., Abdu et al., 1973, 2005; Nishino et al., 2002]. The particle precipitation results in the enhanced ionospheric conductivity at the altitude of D- and E-region due to increase of ionization during both the quiet and disturbed periods suggested by observations of the Ionosonde, riometer, and VLF radio propagation [e.g., Abdu et al., 1973; Nishino et al., 2002]. Abdu et al. [1998, 2003a, b] reported that the ionospheric conductivity tends to be more enhanced during the disturbed periods than during the quiet ones. However, the present analysis result showed that the ratio (SMA/OKI) of the PRI amplitude is almost the same as that of the height-integrated conductivity derived from the IRI-2007 model. Since this model does not include the effect of the high-energy particle precipitation, this fact suggests that the effect of the reduced magnetic field intensity plays

a major role in the enhancement of the ionospheric conductivity in the SAA region. This effect should be clarified in future work by investigating dependence of the PRI and PPI/Stepwise amplitudes on geomagnetic activity together with the analysis of high-energy particles obtained from satellites at the ionospheric altitude.

6. Conclusion

Occurrence features of the preliminary impulse (PI) of geomagnetic sudden commencement (SC) in the South Atlantic Anomaly (SAA) and Pacific Ocean regions from the low latitude (dip latitude: less than 38°) to the dip equator were investigated using the long-term magnetic field data obtained from the CPMN and NSWMM magnetometer networks. The occurrence features of the preliminary reverse impulse (PRI) and preliminary positive impulse (PPI) are summarized below.

1. The PRI and PPI/Stepwise signatures near the dip equator tended to appear dominantly with the peak value of more than 80 % in the daytime (05-19 h, MLT) and nighttime (19-05 h, MLT) sectors, respectively. The occurrence rate tended to decrease with increase of the dip latitude. The occurrence features of the equatorial PRI and PPI/Stepwise signatures did not show a remarkable difference in between the Pacific

Ocean (PON: dip latitude = 1.01° , YAP: dip latitude = 3.29°) and SAA (ANC: dip latitude = 1.43° , SLZ: dip latitude = -2.96°) regions.

2. Magnetic local time dependence of the equatorial PRI amplitude at PON and SMA showed a significant enhancement in the daytime sector with the peak value of 7.7 nT around 10 h (MLT). The distribution of the PRI amplitude in the Pacific Ocean (PON) region indicated almost the same feature as that in the and SAA (ANC) region.
3. The occurrence rate of the low-latitude PRI and PPI/Stepwise signatures became the maximum around noon in both the Pacific Ocean (OKI: dip latitude = 37.97°) and SAA (SMA: dip latitude = -34.35°) regions. This distribution was almost the same tendency as that in the equatorial region. The occurrence rate at SMA was enhanced significantly with its peak value of about 80 %. This peak value was about twice as large as that at OKI in the Pacific Ocean region.
4. The distribution of the low-latitude PRI amplitude at SMA showed a significant enhancement in the daytime sector (06-18 h, MLT), compared with that at OKI. The peak value around noon at SMA was 3.0 times larger than that at OKI. This result suggests that the PRI amplitude tended to be enhanced near the center of the SAA region.
5. The low-latitude PRI signature at OKI appeared dominantly in the daytime (09-16 h,

MLT) sector with the averaged occurrence rate of 25 % in spite of the low-latitude region of more than 15° (dip latitude). The occurrence feature of the PRI in the low-latitude region is quite different from that reported by the past studies [e.g., Matsushita, 1962; Araki, 1977]. However, the distribution of the PRI amplitude gave was a peak value of 0.51 nT around noon, and the value was relatively small. Therefore, the significant enhancement of the PRI occurrence in the low latitude can be considered as a significant improvement of the magnetometer with high accuracy and digitization of the observation data.

6. The calculation result of the IRI-2007 and NRLMSISE-00 models showed a significant enhancement of the $\sigma_{\theta\theta}$, $\sigma_{\theta\phi}$, and $\sigma_{\phi\phi}$ conductivities in the SAA region, where the ambient magnetic field decreases to a half value of the Pacific Ocean region. The ratio of the height-integrated $\Sigma_{\phi\phi}$ conductivities (SMA/OKI) was nearly the same as that of the PRI amplitude ratio. The difference value was 0.5 of 2.5-3.6 around the noon sector (08-16 h, MLT), which corresponds to 14-20 % of the conductivity ratio for each magnetic local time. This result suggests that the weakness of the ambient magnetic field intensity in the SAA region leads to the significant enhancement of the ionospheric conductivities.

Acknowledgements

This work has been supported by the GEMSIS project of Solar-Terrestrial Environment Laboratory in Nagoya University. The authors (Y. Nishimura and Y. Tsuji) are also supported by a grant from Research Fellowship of the Japan Society for the Promotion of Science for Young Scientists. We would like to thank M. A. Abdu at INPE, P. Hattori at the USGS/Guam Magnetic Observatory, U.S. NOAA/Weather Service Office at Yap and Ryukyu University for their help in operating the NICT space weather monitoring magnetometers at Guam, Yap, Okinawa, Sao Luis and Santa Maria, respectively. We also used ASY/SYM index obtained from WDC for Geomagnetism, Kyoto. We acknowledge A. Lazarus, A. Szabo and R.P. Lepping for the IMF-8 Solar Wind and MAG data, L. Frank and S. Kokubun for the Geotail CPI and MGF data, D. J. McComas and N. F. Ness for the ACE SWEPAM and MAG data, and R. Lin and R. Lepping for the Wind 3DP and MFI data provided through CDAWeb, respectively.

References

- Abdu, M. A., S. Ananthkrishnan, E. F. Coutinho, B. A. Krishnan, and E. M. da S. Reis, Azimuthal drift and precipitation of electrons into the South Atlantic geomagnetic anomaly during a SC magnetic storm, *J. Geophys. Res.*, **78**, 5830-5836, 1973.
- Abdu, M. A., P. T. Jayachandran, J. MacDougall, J. F. Cecile, and J. H. A. Sobral, Equatorial F region zonal plasma irregularity drifts under magnetic disturbances, *Geophys. Res. Lett.*, **25**, 4137-4140, 1998.
- Abdu, M. A., I. S. Batista, H. Takahashi, J. W. MacDougall, J. H. A. Sobral, A. F. Medeiros, and N. B. Trivedi, Magnetospheric disturbance induced equatorial plasma bubble development and dynamics: a case study in Brazilian sector, *J. Geophys. Res.*, **108**, 1449, doi:10.1029/2002JA009285, 2003a.
- Abdu, M. A., J. W. MacDougall, I. S. Batista, J. H. A. Sobral, and P. T. Jayachandran, Equatorial evening pre-reversal electric field enhancement and sporadic E layer disruption: a manifestation of E and F region coupling, *J. Geophys. Res.*, **108**, 1257, doi:10.1029/2002JA009721, 2003b.
- Abdu, M. A., I. S. Batista, A. J. Carrasco, and C. G. M. Brum, South Atlantic magnetic

- anomaly ionization: A review and a new focus on electrodynamic effects in the equatorial ionosphere, *J. Atmos. Solar-Terr. Phys.*, **67**, 1643-1657, 2005.
- Araki, T., Global structure of geomagnetic sudden commencements, *Planet. Space Sci.*, **25**, 373-384, 1977.
- Araki, T., A physical model of the geomagnetic sudden commencement, *AGU Geophys. Monogr.*, **81**, 183-200, 1994.
- Araki, T., H. Allen, and Y. Araki, Extension of a polar ionospheric current to the nightside equator, *Planet. Space Sci.*, **33**, 11-16, 1985.
- Araki, T., K. Funato, T. Iguchi, and T. Kamei, Direct detection of solar wind dynamic pressure effect on ground geomagnetic field, *Geophys. Res. Lett.*, **20**, 775-778, 1993.
- Araki, T., K. Keika, T. Kamei, H. Yang, and S. Alex, Nighttime enhancement of the amplitude of geomagnetic sudden commencements and its dependence on IMF-Bz, *Earth planets Space*, **58**, 45-50, 2006.
- Araki, T., S. Tsunomura, and T. Kikuchi, Local time variations of the amplitude of geomagnetic sudden commencements (SC) and SC-associated polar cap potential, *Earth Planets Space*, **61**, e13-e16, 2009.
- Bilitza, D., and B. Reinisch, International Reference Ionosphere 2007: Improvements and

new parameters, *Adv. Space Res.*, **42**, 4, 599-609, 2008.

Chi, P. J., C. T. Russell, J. Raeder, E. Zesta, K. Yumoto, H. Kawano, K. Kitamura, S. M. Petrinec, V. Angelopoulos, G. Le, and M. B. Moldwin, Propagation of the preliminary reverse impulse of sudden commencements to low latitudes, *J. Geophys. Res.*, 106, 18857-18864, 2001.

Chi, P. J., D. H. Lee, and C. T. Russell, Tamao travel time of sudden impulses and its relationship to ionospheric convection vortices, *J. Geophys. Res.*, 101, A08205, doi:10.1029/2005JA011578, 2006.

Fujita, S., T. Tanaka, T. Kikuchi, K. Fujimoto, K. Hosokawa, and M. Itonaga, A numerical simulation of the geomagnetic sudden commencement: 1. Generation of the field-aligned current associated with the preliminary impulse, *J. Geophys. Res.*, **108**, 1416, doi:10.1029/2002JA009407, 2003a.

Fujita, S., T. Tanaka, T. Kikuchi, K. Fujimoto, and M. Itonaga, A numerical simulation of the geomagnetic sudden commencement: 2. Plasma process in the main impulse, *J. Geophys. Res.*, **108**, 1417, doi:10.1029/2002JA009763, 2003b.

Han D. S., and Q. Li, Geomagnetic sudden commencement at the dawn-time dip equator, *Earth Planes Space*, **60**, 607-612, 2008.

Hirono, M., A theory of diurnal magnetic variations in equatorial regions and conductivity of the ionosphere E region, *J. Geomagn. Geoelectr.*, **4**, 7–21, 1952.

Iyemori, T., Storm-time magnetospheric currents inferred from mid-latitude geomagnetic field variations, *J. Geomag. Geoelectr.*, **42**, 1249-1265, 1990.

Iyemori, T., and D. R. K. Rao, Decay of the Dist field of geomagnetic disturbance after substorm onset and its implication to storm-substorm relation, *Ann. Geophys.*, **14**, 608-618, 1996.

Kikuchi, T., Evidence of transmission of polar electric fields to the low latitude at times of geomagnetic sudden commencements, *J. Geophys. Res.*, **91**, 3101-3105, 1986.

Kikuchi, T., and T. Araki, Transient response of uniform ionosphere and preliminary reverse impulse of geomagnetic storm sudden commencement, *J. Atmos. Terr. Phys.*, **41**, 917–925, 1979a.

Kikuchi, T., and T. Araki, Horizontal transmission of the polar electric field to the equator, *J. Atmos. Terr. Phys.*, **41**, 927–936, 1979b.

Kikuchi, T., and T. Araki, Preliminary positive impulse of geomagnetic sudden commencement observed at dayside middle and low latitudes, *J. Geophys. Res.*, **90**, 12,195–12,200, 1985.

Kikuchi, T., T. Ishimine, and H. Sugiuchi, Local time distribution of HF Doppler frequency deviations associated with storm sudden commencements, *J. Geophys. Res.*, **90**, 4389–4393, 1985.

Kikuchi, T., T. Araki, H. Maeda, and K. Maekawa, Transmission of polar electric fields to the Equator, *Nature*, **273**, 650–651, 1978.

Kikuchi, T., S. Tsunomura, K. Hashimoto, and K. Nozaki, Field-aligned current effects on midlatitude geomagnetic sudden commencements, *J. Geophys. Res.*, **106**, 15555–15565, 2001.

Kikuchi, T., K. Hashimoto, and K. Nozaki, Penetration of magnetospheric electric fields to the equator during a geomagnetic storm, *J. Geophys. Res.*, **113**, A06214, doi:10.1029/2007JA012628, 2008.

Kokubun, S., Characteristics of storm sudden commencement at geostationary orbit, *J. Geophys. Res.*, **88**, 10025–10033, 1983.

Kuwashima, M., and H. Fukunishi, Local time asymmetries of the SSC-associated hydromagnetic variations at the geosynchronous altitude, *Planet. Space Sci.*, **33**, 711–720, 1985.

Macdonald, W. M., and M. Walt, Diffusion of electrons in the Van Allen radiation belts, 2,

- particles with mirroring points at low altitude, *J. Geophys. Res.*, **67**, 5025-5035, 1962.
- Matsushita, S., On geomagnetic sudden commencements, sudden impulses, and storm durations, *J. Geophys. Res.*, **67**, 3753–3777, 1962.
- Nagata, T., Distribution of SC* of magnetic storms, *Rep. Ionos. Space Res. Jpn.*, **6**, 13–30, 1952.
- Nagata, T., and S. Abe, Notes on the distribution of SC* in high latitudes, *Rep. Ionos. Space Res. Jpn.*, **9**, 33-44, 1955.
- Nishino, M., K. Makita, K. Yumoto, F. S. Rodrigues, N. J. Schuch, and M. A. Abdu, Unusual ionospheric absorption characterizing energetic electron precipitation into the South Atlantic magnetic anomaly, *Earth Planets Space*, **54**, 907-916, 2002.
- Picone, J. M., A. E. Hedin, D. P. Drob, and A. C. Aikin, NRLMSISE-00 empirical model of the atmosphere: Statistical comparisons and scientific issues, *J. Geophys. Res.*, **107**, 1468, doi:10.1029/2002JA009430, 2002.
- Rastogi, R. G., and N. S. Sastri, On the occurrence of ssc (- +) at geomagnetic observatories in India, *J. Geomagn. Geoelectr.*, **26**, 529-537, 1974.
- Russell, C. T., M. Ginskey, S. Petrinec, and G. Le, The effect of solar wind dynamic pressure changes on low and mid-latitude magnetic records, *Geophys. Res. Lett.*, **19**,

1227-1230, 1992.

Saito, T., K. Yumoto, and Y. Koyama, Magnetic pulsation Pi2 as a sensitive indicator of magnetospheric substorm, *Planet. Space Sci.*, **24**, 1025-1029, 1976.

Sastri, J. H., Penetration electric fields at the nightside dip equator associated with the main impuse of the storm sudden commencement of 8 July, 1991, *J. Geophys. Res.*, **107**, 1448, doi:10.1029/2002JA009453, 2002.

Sastri, J. H., K. Yumoto, J. V. S. V. Rao, and R. Subbiash, On the nature of response of dayside equatorial geomagnetic H-field to sudden magnetospheric compressions, *J. Atoms. Solar-Terr. Phys.*, **68**, 1642-1652, 2006.

Shinbori, A., T. Ono, M. Iizima, and A. Kumamoto, SC related electric and magnetic field phenomena observed by the Akebono satellite inside the plasmasphere, *Earth Planet Space*, **56**, 269-282, 2004.

Shinbori, A., T. Ono, M. Iizima, A. Kumamoto, and Y. Nishimura, Enhancements of magnetospheric convection electric field associated with sudden commencements in the inner magnetosphere and plasmasphere regions, *Adv. Space Res.*, **38**, 1595-1607, 2006.

Shinbori, A., Y. Tsuji, T. Kikuchi, T. Araki and S. Watari, Magnetic latitude and local time dependence of the amplitude of geomagnetic sudden commencements, *J. Geophys. Res.*,

114, A04217, doi:10.1029/2008JA013871, 2009.

Slinker, S. P., J. A. Fedder, W. J. Hughes, W. J. Lyons, and J. G. Lyons, Response of the ionosphere to a density pulse in the solar wind: simulation of traveling convection vortices, *Geophys. Res. Lett.*, **26**, 3549-3552, 1999.

Tamao, T., Hydromagnetic interpretation of geomagnetic SSC*, *Rep. Ionos. Space Res. Jpn.*, **18**, 16–31, 1964.

Trivedi, N. B., M. A. Abdu, B. M. Pathan, S. L. G. Dutra, N. J. Schuch, J. C. Santos, and L. M. Barreto, Amplitude enhancement of SC(H) events in the South Atlantic anomaly region, *J. Atmos. Solar-Terr. Phys.*, **67**, 1751-1760, 2005.

Tsunomura, S., On the polarity of SSC and SI observed in low latitudes, *Mem. Kakioka Mag. Obs.*, **26**, 15–35, 1995.

Tsunomura, S., Characteristics of geomagnetic sudden commencement observed in middle and low latitudes, *Earth Planets Space*, **50**, 755–772, 1998.

Tsunomura, S., Numerical analysis of global ionospheric current system including the effect of equatorial enhancement, *Ann. Geophys.*, **17**, 692–706, 1999.

Tsunomura, S., On the contribution of global scale polar-originating ionospheric current systems to geomagnetic disturbances in middle and low latitudes, *Mem. Kakioka Mag.*

Obs., **28**, 1–79, 2000.

Tsunomura, S., and T. Araki, Numerical analysis of equatorial enhancement of geomagnetic sudden commencement, *Planet. Space Sci.*, **32**, 599–604, 1984.

Tsurutani, B. T., and G. S. Lakhina, Some basic concepts of wave particle interactions in collision less plasmas, *Rev. Geophys.*, **35**, 491-501, 1997.

Vernov, S. N., E. V. Gorchakov, P. I. Shavrin, and K. N. Sharvina, Terrestrial corpuscular radiation and cosmic rays, *Space Sci. Rev.*, **7**, 490-533, 1967.

Wilken, B., C. K. Goertz, D. N. Baker, P. R. Higbie and T. A. Fritz, The SSC on July 29, 1977 and its propagation within the magnetosphere, *J. Geophys. Res.*, **87**, 5901-5910, 1982.

Yamada, Y., M. Takeda, and T. Araki, Occurrence characteristics of the preliminary impulse of geomagnetic sudden commencement detected at middle and low latitudes, *J. Geomagn. Geoelectri.*, **49**, 1001-1012, 1997.

Yumoto, K., and the CPMN Group, Characteristics of Pi 2 magnetic pulsations observed at the CPMN stations: A review of the STEP results, *Earth Planets Space*, **53**, 981-992, 2001.

Figure Captions

Figure 1. Waveform of geomagnetic field variations of the H-component during SC occurred at 16:47:45 (UT) on 21 October, 2001. The time interval is 7 minutes from 16:46 to 16:53 (UT). The vertical dashed lines in both the panels give the onset time of SC, while the dotted-dashed line in the lower panel indicates the peak amplitude of the PPI/Stepwise signature associated with SC. The upper and lower panels indicate the H-component data with time resolution of 1 second obtained at ANC, EUS and SMA near the SAA region and at OKI, GAM, CEB, YAP, and PON in the Pacific Ocean region, respectively.

Figure 2. Difference of geomagnetic field variations of the H-component between GAM, CEB, YAP, PON and OKI during SC. The format of this figure is the same as that of the panel (b) in Figure 1. There can be seen an abrupt increase of the H-component with its duration time of about 1 minute at GAM, YAP and PON at the onset of SC.

Figure 3. Waveform of geomagnetic field variations of the H-component during SC occurred at 06:25:50 (UT) on 4 November, 2003. The time interval is 7 minutes from 06:24 to 06:31 (UT). The

vertical dashed lines in both the panels give the onset time of SC, while the dotted-dashed line in the upper panel indicates the peak amplitude of the PPI/Stepwise signature associated with SC. The upper and lower panels indicate the H-component data with time resolution of 1 second obtained at SLZ, EUS and SMA near the SAA region and at OKI, CEB, YAP, and PON in the Pacific Ocean region, respectively.

Figure 4. Occurrence rate of the PRI and PPI/Stepwise signatures during SCs detected at each station as a function of magnetic local time. The left and right panels are that of the Pacific Ocean and SAA regions, respectively, in a dip latitude range from 1.0° to 38° . The red (PRI), blue (PPI) and green (Non) colors correspond to the PRI, PPI/Stepwise and unclear signatures, respectively. The station name and dip latitude are shown in the top of each panel.

Figure 5. Average distribution of the PRI amplitude in the Pacific Ocean and SAA regions near the dip equator (PON-ANC) (panel (a)) and off equator (OKI-SMA) (panel (b)) as a function of magnetic local time. The red and green lines indicate the averaged PRI amplitude detected in the Pacific Ocean and SAA regions, respectively.

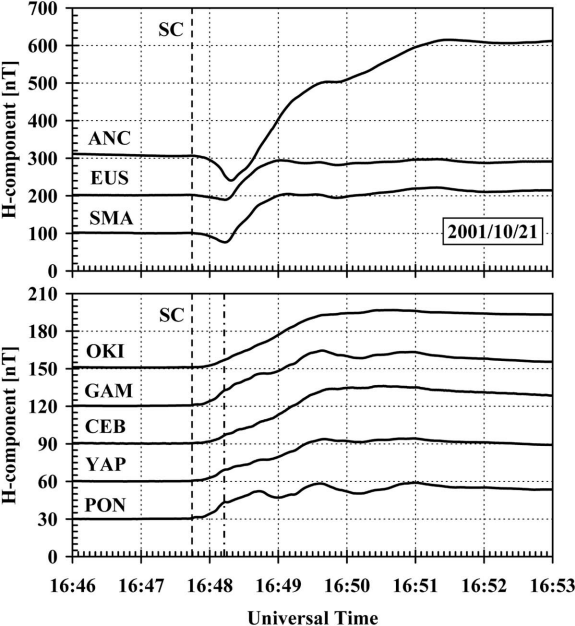
Figure 6. Altitude profiles of ionospheric conductivity at OKI (a) and SMA (b), electron-neutral, ion-neutral collision, electron, NO^+ , O^+ ion cyclotron angular frequencies at OKI (c) and SMA (d) derived from NRLMSISE-00 and IRI-2007. The vertical axes in each panel are altitude in a range from 50 to 250 km. In the panels (a) and (b), the red, blue, and green lines indicate the $\sigma_{\theta\theta}$, $\sigma_{\theta\phi}$, and $\sigma_{\phi\phi}$ conductivities, respectively. The labels ‘Nu_NO+n’, ‘Nu_O+n’, ‘Nu_en’, ‘ Ω_{c_e} ’, ‘ $\Omega_{c_{\text{NO}^+}}$ ’ and ‘ $\Omega_{c_{\text{O}^+}}$ ’ stand for the collision frequencies between the neutral particles and ions (NO^+ , O^+) and electron, and the cyclotron angular frequencies of electron, NO^+ and O^+ ions, respectively.

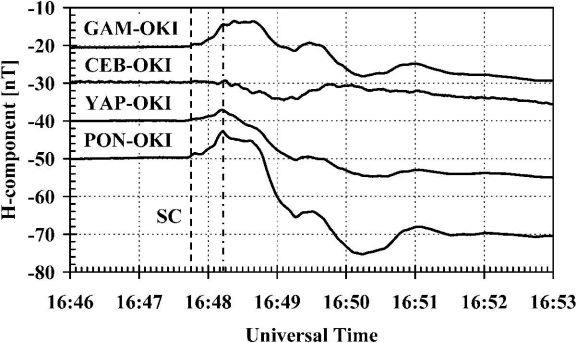
Figure7. Ratios (ANC/PON and SMA/OKI) of the daytime PRI amplitude and height-integrated $\Sigma_{\phi\phi}$ conductivity as a function of magnetic local time. In each panel, the red and green lines indicate the height-integrated conductivity and PRI amplitude ratios.

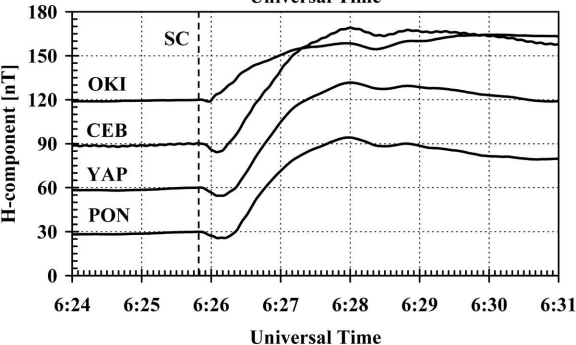
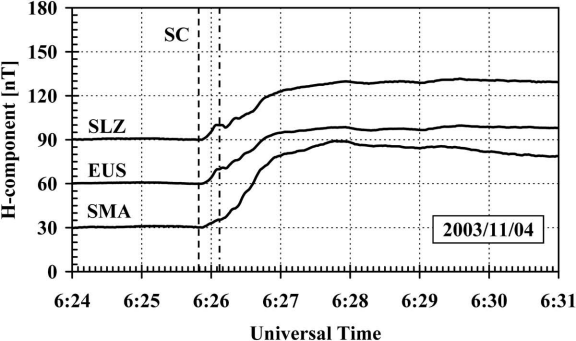
Table 1. Lists of magnetogram station, analysis period and SC events

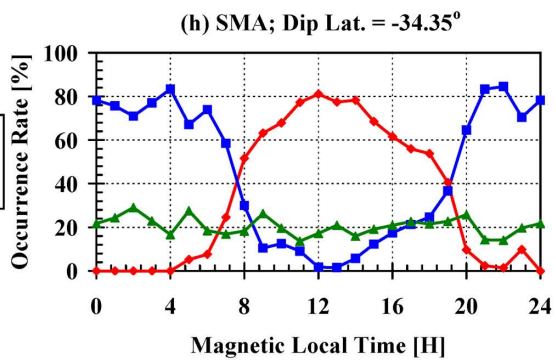
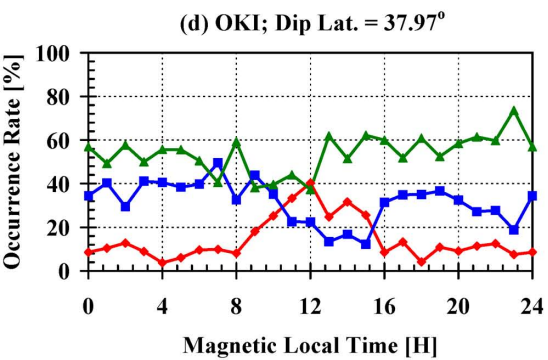
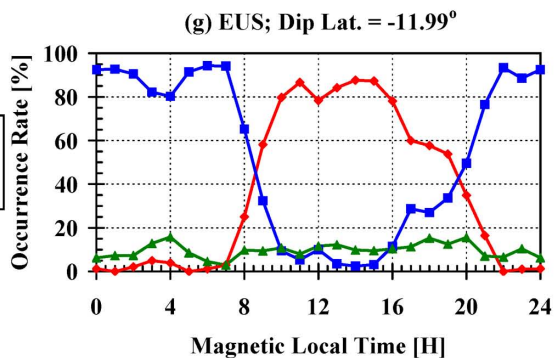
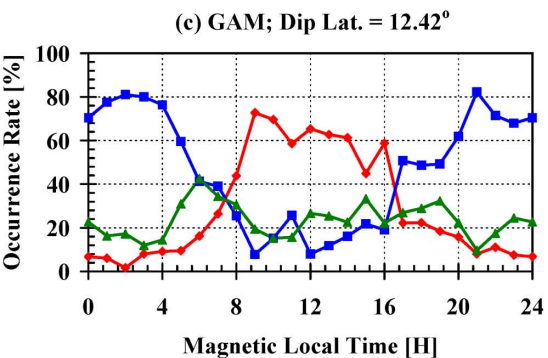
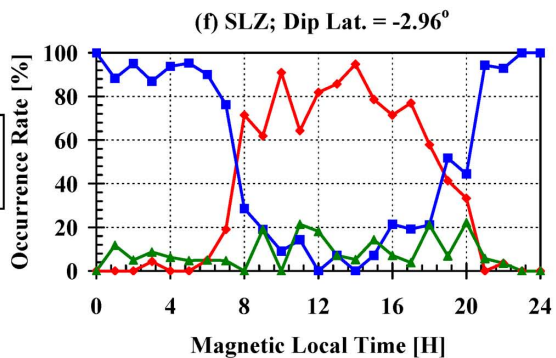
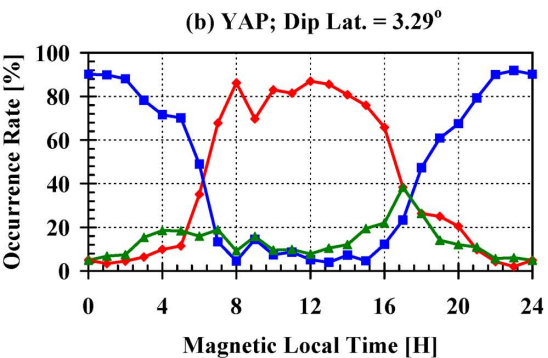
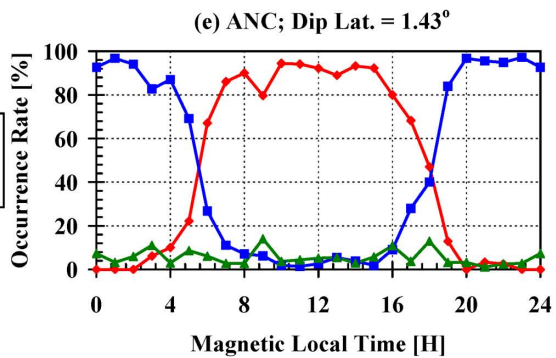
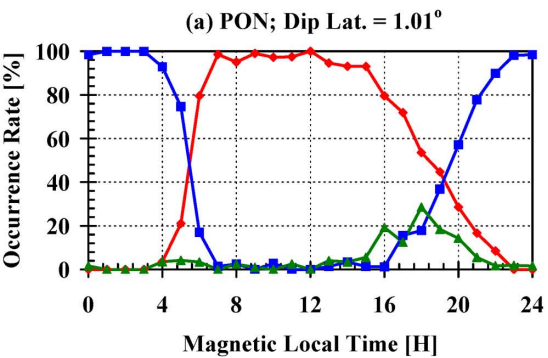
Station	Dip LAT. [deg]	GMLAT. [deg]	GMLONG. [deg]	Analysis period	Number of SC events
Ancon (ANC)	1.43	3.10	354.66	1996/01-2006/10	2046
Sao Luis (SLZ)	-2.96	6.49	27.75	2002/12-2007/04	462
Eusebio (EUS)	-11.99	4.72	33.41	1996/01-2006/01	2104
Santa Maria (SMA)	-34.35	-19.82	13.31	1998/04-2008/09	1692
Okinawa (OKI)	37.97	16.87	198.41	1996/04-2008/10	2028
Guam (GAM)	12.42	5.22	215.64	1996/01-2003/07	1666
Cebu (CEB)	5.79	0.85	195.27	1998/08-2005/06	1599
Yap (YAP)	3.29	0.38	209.21	1998/09-2008/09	1921
Pohnpei (PON)	1.01	0.27	229.44	1997/03-2004/05	1631

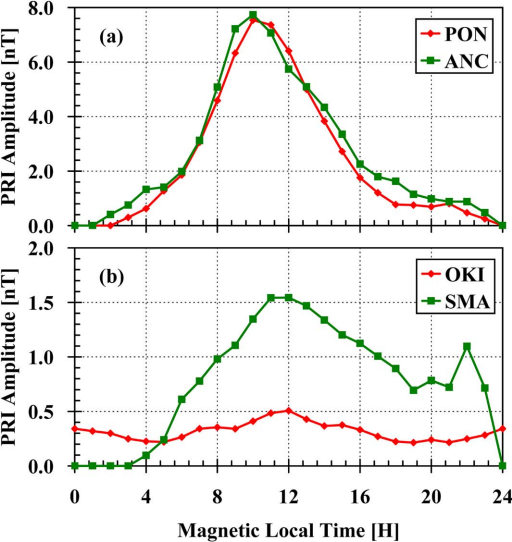
Table 1



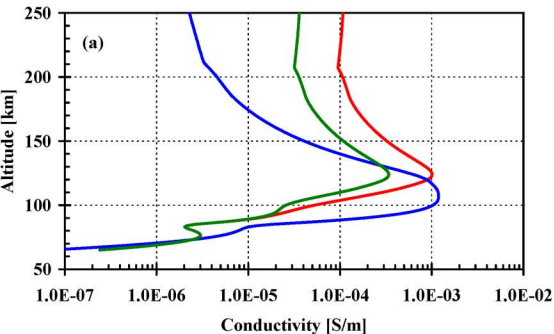




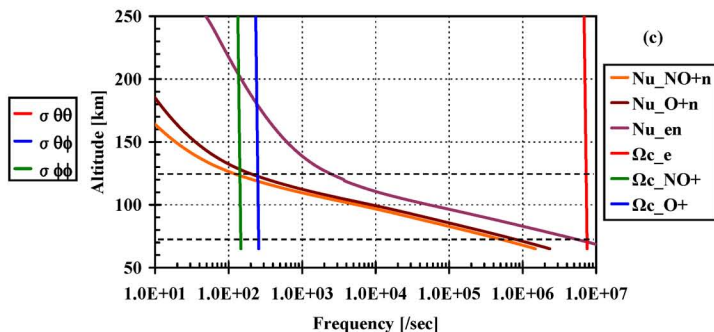




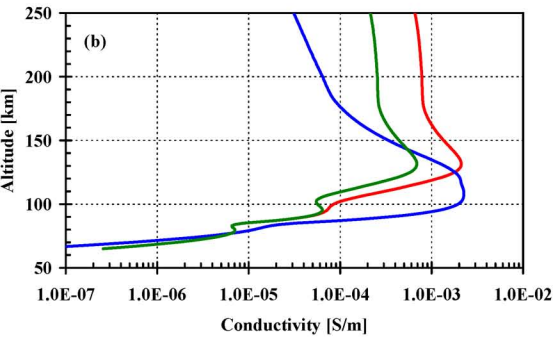
Altitude Profile of Conductivity at OKI



Altitude Profile of Collision and Cyclotron Frequencies at OKI



Altitude Profile of Conductivity at SMA



Altitude Profile of Collision and Cyclotron Frequencies at SMA

